Silica Surface-Modification for Tailoring the Charge Trapping Properties of PP/POE Based Dielectric Nanocomposites for HVDC Cable Application

XIAOZHEN HE [ORCID][1]**, (Member, IEEE), ILKKA RYTÖLUOTO**[2]**, RAFAL ANYSZKA**[1]**, (Member, IEEE), AMIRHOSSEIN MAHTABANI**[1]**, (Member, IEEE), EETTA SAARIMÄKI**[2]**, KARI LAHTI**[3]**, MIKA PAAJANEN**[2]**, WILMA DIERKES**[1]**, AND ANKE BLUME**[1]

[1]Elastomer Technology and Engineering Group, Department of Mechanics of Solids, Surfaces and Systems (MS3), Faculty of Engineering Technology, University of Twente, 7500 AE, Enschede, The Netherlands
[2]VTT Technical Research Centre of Finland Ltd., 33101 Tampere, Finland
[3]Research Group on High Voltage Engineering, Tampere University, 33720 Tampere, Finland

Corresponding authors: Wilma Dierkes (w.k.dierkes@utwente.nl), Xiaozhen He (x.he@utwente.nl), and Rafal Anyszka (r.p.anyszka@utwente.nl)

This work was supported by the European Union's Horizon 2020 Research and Innovation Program under Grant 720858.

ABSTRACT This paper focuses on novel insulation polypropylene/poly(ethylene-co-octene) (PP/POE) nanocomposites for High Voltage Direct Current (HVDC) cable application. The composites contain silica modified by a solvent-free method using silanes differing in polarity and functional moieties. Thermogravimetric Analysis and Fourier Transform Infrared Spectroscopy showed that the solvent-free method is an effective way to modify silica by silanes. Silica/PP/POE nanocomposites were prepared in a mini twin-screw compounder, and the effect of silica on crystallization, dispersibility and dielectric properties of the samples was investigated. Differential Scanning Calorimetry results showed that the unmodified and modified silicas acted as nucleation agents and increased the onset of the crystallization temperature of the polymeric matrix. Scanning Electron Microscopy images showed that the silica is mostly located in the PP phase matrix. For the PP/POE nanocomposites filled with unpolar silica, a higher trap density (measured by Thermally Stimulated Depolarization Current, TSDC) was found; this might be caused by the larger interfacial area due to a better dispersion of the unpolar silica in the polymeric matrix. Polar silicas introduce deeper traps than the unpolar ones, which is most likely due to the hetero-atom introduction. Nitrogen atoms were found to have the strongest effect on the charge trapping properties. According to these results, amine-modified silica is a promising candidate for PP/POE nanocomposites for HVDC cable applications.

INDEX TERMS PP/POE, nanosilica, surface modification, dispersibility, crystallization behavior, trap distribution, HVDC cable.

I. INTRODUCTION

Thermoplastic dielectric composites containing nanofillers have attracted a lot of interest in the field of high voltage insulation field [1]–[3]. It is widely accepted that the large interface formed between a nanofiller and a polymer matrix plays a critical role in the high voltage dielectric properties of nanocomposites [4]–[6].

However, one of the general problems in the preparation of nanocomposite preparation is to achieve good dispersion of the nanofillers in the polymer matrix. For instance, it is

The associate editor coordinating the review of this manuscript and approving it for publication was Boxue Du [ORCID].

reported that the dc conductivity of LDPE increases remarkably with higher nanofiller loading (>3 phr) than the one filled with a lower amount of nanofiller (1 to 3 phr) duo to extensive nanofiller agglomerate formation [7]. In principle, improving the performance of a nanodielectric requires good dispersion of the nanofiller, which results in larger interface area between the nanofiller and polymer.

Although a better dispersion of nanofillers is crucial, the type of surface functionalization of nanofillers is also very important from the point of view of dielectric properties. Incorporation of functional polar groups on the nanofiller surface can positively alter the dielectric properties of a nanocomposite. It is reported that the introduction of

polar groups (amine) onto a nanoparticle surface improves the breakdown strength of polyethylene nanocomposites due to the modified electrical features (e.g. charge trapping) at the polymer-nanoparticle interface [8]. Modified silica containing polar chlorine atoms can suppress the space charge accumulation of in crosslinked polyethylene (XLPE) nanocomposites, due to a change in the spherulites size distribution [9]. Furthermore, nanofillers grafted with π-conjugated surface ligands can act as electron trap to alter the avalanche breakdown of silica-epoxy nanocomposites [10].

The dielectric performance of an insulation material is associated with charge trapping/detrapping phenomena. The temperature- and field-dependent transportation of charges in nanocomposites varies with the polarity and morphology of the polymeric matrix, the type, size and dispersion of the nanofillers, and and the tailored surface properties of the nanofillers [11], [12]. Therefore, the influence of modified nanofillers having different surface polarities on the charge trapping properties of the dielectric materials is studied. Previously, the introduction of different polar functional groups on the silica surface resulted in significant differences in charge trapping properties of the nanocomposites [13], [14]. Following up our previous study [14], the current research not only covers the phenomenon of charge trapping properties, but also includes various characterization methods to investigate the mechanism of it.

In general, silica-silane modification in most cases is performed in a solvent at various temperatures [15]–[17]. This enables utilization of various functional silanes and versatile conditions resulting in a good control of the silane deposition on the silica surface. However, this also causes an environmental burden by the solvent waste that needs to be properly recycled or disposed of. Therefore, this paper aims also to develop a new solvent-free method for silane modification of silica nanoparticles.

As one requirement of this new development was sustainability and recyclability, polypropylene (PP) and polyolefin (POE) based materials were chosen for the matrix. The currently used cross-linked polyethylene cannot be recycled and reused due to its polymer network. Switching to PP and POE allows to develop a recyclable HVDC cable insulation material with less environment impact. Blending PP with a polyolefin can improve the flexibility of the former polymer, and the addition of the nanofiller can result in a significant improvement of the thermoplastic dielectric properties. This can further increase the potential to be used as HVDC cable insulation material [1].

In summary, the objectives of this study are:

1) Developing an easy-to-upscale solvent-free method to tailor silica surface properties

2) Investigating the influence of a silica surface modification on the performance (crystallization, dispersibility and charge trapping dielectric behavior) in PP/POE nanocomposites.

II. MATERIALS AND CHARACTERIZATIONS

A. MATERIALS
Fumed silica (Aerosil 200) was obtained from Evonik Industries Germany. The 3-glycidyloxypropyl trimethoxysilane, aminopropyltriethoxy silane and isocyanatopropyltriethoxy silane were purchased from Sigma-Aldrich, US. All other silanes (trimethylethoxysilane, dimethyldiethoxysilane, methyltriethoxysilane, vinyldimethylethoxysilane, phenyldimethylethoxysilane, mercaptopropyltrimethoxysilane) were purchased from Abcr GmbH, Germany, as were trifluoroacetic acid and ammonia. A blend of polypropylene (PP) and poly (ethylene-co-octene) (POE) was used as the polymeric matrix.

The silane modification of silica is described in Section B. The different nanocomposites destined for high voltage DC (HVDC) cable insulation were prepared by melt-blending of 1wt% of the reference silica (unmodified) or the modified silicas with a PP/POE = 55:45 blend and 0.3 wt% of antioxidant using a a twin-screw micro extruder, type Haake Mini-Lab Rheomix CTW5 (Thermo Fisher Scientific, Waltham, Massachusetts, USA). The compounding was performed at a temperature of 230 °C using a screw speed of 100 rpm for 4 minutes (min). After melt-blending, the nanocompounds were immediately transferred in molten-state to an injection moulding system Haake MiniJet Pro Piston Injection Moulding System (Thermo Fisher Scientific, Waltham, Massachusetts, USA) and moulded into thin sheets with dimensions of $26 \times 26 \times 0.5$mm.

B. CHARACTERIZATION OF SILICA
Information on the chemical composition and structure of the surface of the unmodified and modified silicas was obtained by Fourier Transform Infrared Spectrometry (FTIR; Perkin Elmer – Spectrum 100 series) with the resolution of 0.1% in the range of 400 to 4000 cm-3. Thermogravimetric Analysis thermogravimetric analyzer TGA-7 (Perkin-Elmer, Waltham, Massachusetts, United States) was performed in order to investigate the extent of silanization of the silica. This characterization was done in a synthetic air atmosphere with a heating rate of 20 °C/min. The temperature range was from ambient temperature up to 850 °C. X-ray Photoelectron Spectroscopy (XPS) was conducted by means of a Scanning X-ray Microscope PHI Quantera (Physical Electronics GmbH, Munich, Germany) to check the chemical composition of the silicas. The silica particle morphology was evaluated by Transmission Electron Microscopy (TEM) and Energy Dispersive X-ray analysis (EDX) using a Transmission Electron Microscope CM300ST-FEG 300 kV (Philips, Eindhoven, the Netherlands).

C. CHARACTERIZATION OF SILICA/PP/POE NANOCOMPOSITES
The melting and crystallization properties of the nanocomposites were investigated by differential Scanning Calorimetry (DSC) using a DSC Q2000 (TA Instruments, New Castle,

Delaware, USA). Samples with a weight of around 12-14 mg were placed in a standard aluminum pan. They were first heated from ambient temperature to 230 °C at a rate of 10 °C/min, and kept at this temperature for 5 min to erase any previous thermal history. The samples were then cooled down to −20 °C (40 °C/min) and heated again to 230 °C at a rate of 10 °C/min The crystalline structure was studied by X-ray Diffraction (XRD) spectra using a X'Pert 1 X-ray diffractometer (Philips, Almelo, The Netherlands). Diffraction spectra in the 2θ range from 5° to 37° with a scanning rate of 0.05 °/8 s were collected. Scanning Electron Microscopy (SEM) was done by means of a MERLIN HR-SEM (Zeiss, Oberkochen, Germany).The sample for SEM was prepared in liquid nitrogen without any coating.

The charge trapping properties of the PP/POE nanocomposites were studied by Thermally Stimulated Depolarization Current (TSDC). Circular gold electrodes (diameter 16 mm, thickness 100 nm) were deposited on both sides of the sample sheets by electron-beam evaporation under high vacuum ($< 1 \times 10{-6}$ mbar). The TSDC measurement system consisted of a liquid nitrogen-based temperature control system Novocool (Novocontrol Technologies, Montabaur, Germany), a DC high voltage source 2290E-5 (Keithley Instruments, Cleveland, Ohio, USA) and a sensitive electrometer 6517B (Keithley Instruments, Cleveland, Ohio, USA). The samples were placed in a shielded sample cell equipped with a PT100 temperature sensor (Novocontrol BDS1200HV). The TSDC measurement procedure consisted of the following steps:

1) The samples were heated up to 70 °C and kept stable for 5 min;

A DC electric field of 3 kV/mm was applied for 20 min under isothermal conditions at 70 °C;

3) The samples were rapidly cooled down to −50 °C with the voltage still applied, and kept at this temperature for 5 min for stabilization;

4) The electric field was removed and the samples were short-circuited through an electrometer. The short-circuited samples were maintained at −50 °C for 3 min to allow fast polarization to decay;

5) The samples were linearly heated up to 130 °C with a heating rate of 3 °C/min. Meanwhile, the depolarization current was recorded.

III. RESULTS

A. SOLVENT-FREE MODIFICATION OF SILICA BY SILANES

In this study, trimethylethoxysilane (Fig.1) was chosen as the starting modifying agent, as it has only one ethoxy group and therefore does not suffer from side reactions such as condensation. Two kinds of catalysts, ammonia and trifluoroacetic acid, were used to accelerate the silanization reaction to make it take place at room temperature.

The solvent-free modification method was chosen, as it is more environmentally friendly in comparison to solution methods. It was carried out in a sealed glass jar with a
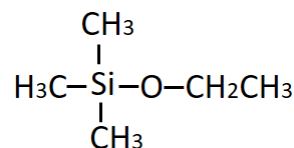

FIGURE 1. Chemical structure of Trimethylethoxysilane.

magnetic stirrer at room temperature for 24 hours. All the modification variants were performed with the same amount of fumed silica (10 g), trimethylethoxysilane (0.98 g), water (0.3 g) and fixed amounts of the catalysts (trifluoroacetic acid (0.2 g) or ammonia (1 g)). After the modification, the product was extracted in a Soxhlet unit with ethanol for 24 hours to remove all contaminants, and afterwards placed in a vacuum oven at a temperature of 80 °C for 24 hours to remove ethanol.

Five different silica modifications were selected:

S – unmodified silica;

SS – silica modified with the silane;

SSW – silica modified with the silane in presence of water;

SSWA – silica modified with the silane in presence water and trifluoroacetic acid;

SSWB – silica modified with the silane in presence water and ammonia (base).

1) THERMO-GRAVIMETRIC ANALYSIS (TGA)

For quantitative analysis of the modification effects, TGA was performed. The results are depicted in Fig.2. The weight loss of the pure silica (S) was 2%; however, in the case of SS and SSW, comparable weight losses of 2.1% and 2.4% respectively were measured. This indicates that there are barely any organic groups chemically attached to the silica surface in case of SS and SSW silicas. After the functionalization in presence of the catalysts, the weight loss increased to 4.1% for SSWA and to 7.2% for SSWB. On the basis of the TGA curves, it can be concluded that solvent free silane modification of silica proceeds successfully only when a catalyst is present, regardles of its nature – acidic or basis. However, the kinetics of thermal decomposition of the samples modified in presence of the acid and of the base varies significantly. The modification performed in presence of ammonia results in a high amount of volatiles and relatively loosely bound surface-deposition; it shows a constant
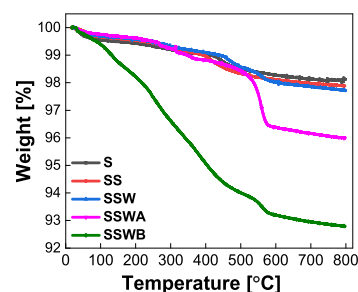

FIGURE 2. TGA results of the unmodified and modified silicas.

decrease of mass from ca. 100 °C to 500 °C. This might be due to the physical adsorption of the base onto the silica surface through hydrogen bonds, which are not stable and will be decomposed at lower temperature.

2) FOURIER TRANSFORM INFRARED (FTIR)

Fourier Transform Infrared (FTIR) analysis was performed on the unmodified silica and modified silica samples. This technique allows to identify organic groups by measuring the absorption of infrared radiation by the sample material within a certain spectrum of wavelengths. The infrared absorption bands are characteristic for certain molecular components and structures.

Fig.3 compares the spectra of unmodified silica (S) and modified silicas (SS, SSW, SSWA and SSWB). A new band in the region of 2963 cm^{-1} appeared after the silane modifications. This band represents the C-H stretching [18] which comes from the trimethylethoxysilane. The stronger the band intensities, the higher the modification effect. As seen in Fig.3, the band became stronger with the addition of the catalysts. These results are in agreement with the results of the TGA analysis, indicating that there is indeed a C-H organic layer covering the silica surface after the solvent-free modification. The reaction mechanism of the silica-silane modification is shown in Fig.4.
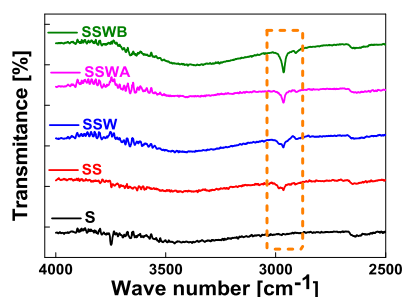

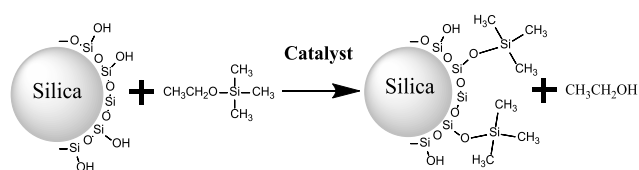**FIGURE 3.** FTIR spectra of the unmodified and modified silicas.

FIGURE 4. Reaction scheme of the solvent-free silica-silane modification.

3) X-RAY PHOTOELECTRON SPECTROSCOPY (XPS)

In order to further evaluate the modification of silica, X-ray Photoelectron Spectroscopy (XPS) was performed on the unmodified silica (S) and modified silicas (SSWA and SSWB). XPS works on the basis of irradiating a material with a beam of X-rays while simultaneously measuring the kinetic energy and number of electrons that escape from the surface (0 to 10 nm) of the analyzed material. Thus, it is

possible to measure the elemental composition of a very thin surface layer in a parts per thousand range. The XPS results are presented in Fig. 5 and TABLE 1. The carbon, oxygen and silicon atom spectra and their content are shown.
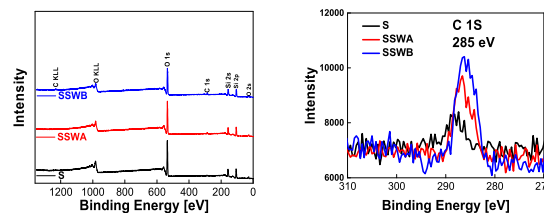

FIGURE 5. XPS spectra of the unmodified (S) and modified silicas (SSWA, SSWB).

TABLE 1. Chemical composition of the surface of unmodified and modified silicas by XPS.

	C	O	Si
S / atom%	1.8	69.2	28.9
SSWA / atom%	5.4	64.6	29.9
SSWB / atom%	8.8	61.7	29.4

Both, SSWA and SSWB, exhibited an increased C1s signal at a binding energy of ca. 280 eV in the XPS spectrum (Fig.5) demonstrating the presence of carbon from the silane molecules. This corresponds to the results obtained from FTIR and TGA measurements. The small carbon signal present in the reference spectra (S) comes from atmospheric contaminations deposited on the silica during sample preparation. The oxygen signal (O1s) originates from the silica structure. The decreased O1s signal for the SSWA and SSWB samples versus the S sample at ca. 530 eV also confirms a successful surface modification. The decreased oxygen content observed in the silane modified silica samples is a result of the presence of the methyl groups, which are bond to a silicone atom in the silane molecule. This increases the amount of carbon in the surface layer of the modified samples covering the amorphous SiO_2 particles.

The silicon signal (Si2p) intensity is similar for unmodified and silane-coated silicas. This is an effect of two simultaneous processes: attachment of silicon atoms with the deposition of silane molecules and covering of the SiO_2 particles. In summary, the effect of enriching the surface layer with silicone atoms seems to be more efficient resulting in a slight increase of the silicone amount (TABLE1). Altogether, TGA, FTIR and XPS proved a successful silica-silane modification via the solvent-free modification.

In conclusion, the solvent-free method is an effective and sustainable approach to perform silica-silane modification using an acidic or alkaline catalyst. In general, the silica modified using the base catalyst (SSWB) exhibit a higher modification level in comparison with the acid catalyzed silica (SSWA). However, the modification performed on SSWB is significantly less thermally stable, based on the TGA results:
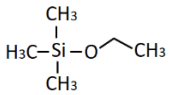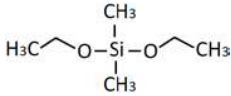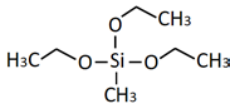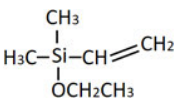
TABLE 2. Silanes from Group I.
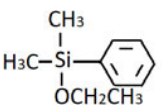
Silane abbreviation	Full name	Structure
TMES	Trimethylethoxy Silane	
DMDES	Dimethyldiethoxy Silane	
MTES	Triethoxymethyl Silane	

TABLE 3. Silanes from Group II.

Silane abbreviation	Full name	Structure
VDMES	Vinyldimethylethoxy Silane	
PDMES	Phenyldimethylethoxy Silane	

TABLE 4. Silanes from Group III.
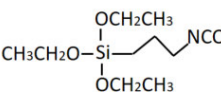
Silane abbreviation	Full name	Structure
HS-silane	Mercaptopropyltrimethoxy Silane	
Epoxy-silane	3-Glycidyloxypropyl trimethoxysilane	
Amino-silane	Aminopropyltriethoxy Silane	
NCO-silane	Isocyanatepropyltriethoxy Silane	

TABLE 5. Recipe for silane–silica solvent free modification.

	Silane/g	Silica/g	Water/g	Acid/g
TMES	1.96			
DMDES	2.46			
MTES	2.94			
VDMES	2.15			
PDMES	2.98	20	0.60	0.40
Epoxy-silane	3.92			
HS-silane	3.25			
NCO-silane	4.10			
Amino-silane	3.67			

the onset of the mass loss of SSWB starts from 100 °C, while it is 500 °C for SSWA. Therefore, trifluoroacetic acid is selected as a catalyst for the silane-silica modification.

B. TAILORING THE SILICA SURFACE WITH DIFFERENT SILANES VIA THE SOLVENT-FREE METHOD

The solvent-free method was performed on fumed silica using 8 different silanes. The investigated silanes were divided into three groups:

I. Aliphatic silanes with different numbers of alkoxy groups (TABLE 2).

II. Hydrocarbon silanes containing delocalized electron clouds (TABLE3).

III. Polar silanes containing hetero elements (nitrogen, sulfur or oxygen) (TABLE 4).

The above classification aims at verifying the effectiveness of the modification by the solvent-free method and at producing different silicas with varied surface properties in order to study their influence on dielectric properties of nanocompos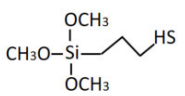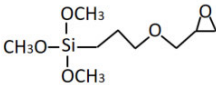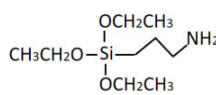ites. For purification, the samples were put into a vacuum oven at 80 °C to remove the residues, instead of extraction and oven drying.

The amount of the silane added for the modification is shown in TABLE 5. It is based on Equation (1):

$$m(silane) = m(silica) * S(silica) * N(Si\text{-}OH) * M(silane)/NA \quad (1)$$

where:

m(silane) = amount of silane used for the solvent-free modification;

m(silica) = 20 g is the amount of silica used for the solvent-free modification;

S(silica) = 200 m^2/g, the specific surface area of the silica;

N(Si-OH) = 2.5 / nm^2, the number of silanol groups on the silica surface per 1 nm^2;

M (silane) = molecular weight of a silane;

NA = 6.022 × 10^{23}, Avogadro constant.

The calculation is based on two assumptions:

1. One silane molecule will react with one silanol group on the silica surface.

2. All the silanol groups on the silica surface will have reacted with the silane.

1) THERMO-GRAVIMETRIC ANALYSIS (TGA)

The TGA curves of the modified silicas are shown in Fig.6 (Group I (a), Group II (b) and Group III (c)). The weight loss attributes to the removal of the molecules from the silica surface. The weight loss below 100 °C results from water and unreacted alkoxy groups present on silica surface which undergo condensation [19]. The breakage of Si-C bonds mostly contributes to the weight loss between 300~450 °C [20]. With increasing temperature, the condensed organic polymer on silica surface starts degradation which leads to the weight loss at temperatures higher than 450 °C [20], [21].
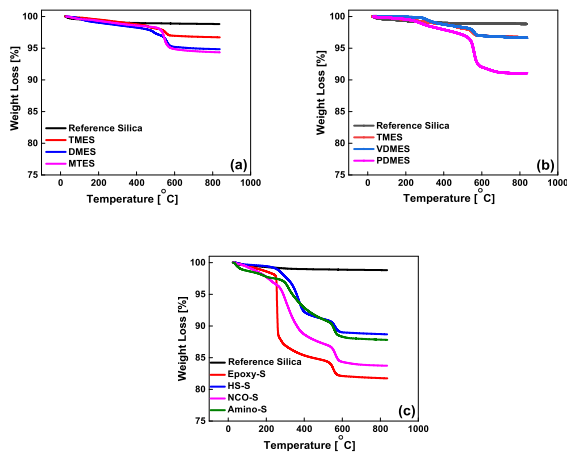
FIGURE 6. TGA curves of unmodified and modified silicas treated with silanes from different groups (Group I (a), Group II (b) and Group III (c)).

Comparing the weight loss of silica modified with the silanes from Group I, it is clear that using molecules containing more than one alkoxy group results in a higher degree of deposition. This is most likely due to a condensation reaction of the alkoxy groups leading to silane oligomerization, thus enhanced surface covering. In Group II, the silica modified with PMDES showed noticeably higher weight loss resulting from the higher molecular weight of the phenyl group of the silane. The silanes with different polar moieties in Group III all have three alkoxy groups and a slightly longer side chain than the one in Group I. This caused a much higher weight loss during the TGA tests as shown in Fig.6. It is worth noting that utilization of the 3-glycidyloxypropyltrimethoxy silane (epoxy-S) and isocyanatepropyltriethoxy silane (NCO-S) for modification resulted in a deposition exceeding 15 % of the treated silica mass. This is an exceptional result in comparison to the state of the art methods presented in the literature, in which the deposition level usually does not exceed 10 % [22]. Higher levels of silica modification usually require a complex, multi-step procedure [23].

To get further quantitative insight into the modification degree of the solvent-free method, the molar amount of grafted silane was calculated based on the Equation (2):

$$Grafted\ amount(mmol/g) = \frac{10^3 W}{M(100 - W)}\ [24] \qquad (2)$$

where:

W = weight difference between the weight at 100 °C and 750 °C;

M = molecular weight of a side chain of a silane.

This equation was introduced by He *et al.* [24]. However, the whole molecular weight of a silane was considered to be equal to M by the authors. This is not accurate considering the mechanism of thermal detachment of the silane molecules from a silica surface (Fig.7). Silane molecules form strong covalent bonds (Si-O-Si) with the silica surface. This bond is very unlikely to break during a TGA test. Instead, at lower temperatures residual alkoxy groups are removed (C-O bond), whereas at higher temperatures breakage of Si-C bond occurs. During water and acid catalyzed silanization, we assume that all the alkoxy groups are hydrolyzed to form silanol groups (Si-O-H). Therefore, only the removal of a side chain of a silane contributes to the weight loss during TGA measurements. This gives a strong indication that the molecular weight of the silane side chain should be taken into consideration in the above equation rather than the whole silane molecular weight. This is also confirmed by other researchers [25].

FIGURE 7. Mechanism of thermal degradation of a silane grafted on silica. (During heating, the unreacted alkoxy groups marked in red will leave firstly; with further increasing temperature, the Si-R' bond of the side chain from the silane marked in green will be broken).

The results of the calculated amount of deposited silanes are shown in Fig.8 (right). They are noticeably different than the TGA total weight losses shown in Fig.8 (left). While the TGA weight loss in Fig.8 (left) exhibited a correlation with the molecular weight of the side chain in the silane,
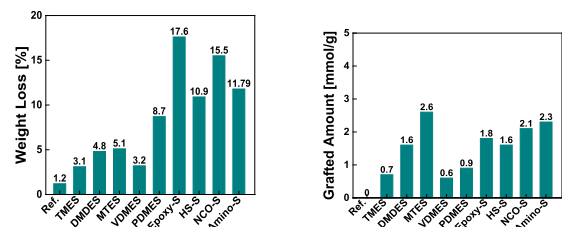
FIGURE 8. The weight loss of the modified silicas (left) and molar amount of grafted silanes on silica surface (right).

the grafted amounts in Fig.8 (right) were more dependent on the number of reactive alkoxy groups.

These results show that there is almost the same amount of silane (in mmol) grafted onto the silica surface when modified with a silane containing only one alkoxy group (0.7 mmol/g of TMES, 0.6 mmol/g of VDMES, 0.9 mmol/g of PDMES). However, the total weight loss of PDMES modified silica gave a much higher value (8.7 %) than the silicas modified with the two other silanes (1.2 % of TMES and 3.2 % of VDMES) due to the much higher molecular mass of the phenyl ring. Furthermore, regarding to the silanes containing three alkoxy groups (MTES, epoxy-silane, HS-silane, NCO-silane and amino-silane), the degree of modification was more or less on the same level (from 1.6 mmol/g to 2.6 mmol/g), while there is a significant difference in the total weight loss results (from 5.1 % to 17.6 %).

In summary, a higher TGA weight loss does not directly equal to a more effective silane modification on the silica surface. To compare the degree of modification, the grafted amount of silane in mmol/g should be calculated. Nevertheless, all the above results show that the solvent-free method is an efficient way to perform silica-silane modification.

2) FOURIER-TRANSFORM INFRARED SPECTROSCOPY (FTIR)

The FTIR spectra of unmodified and modified silicas are shown in Fig.9. The band at 2956 cm^{-1} is attributed to the stretching vibration of C-H [26]. This proves that TMES, DMDES and MTES were successfully grafted onto silica surface.
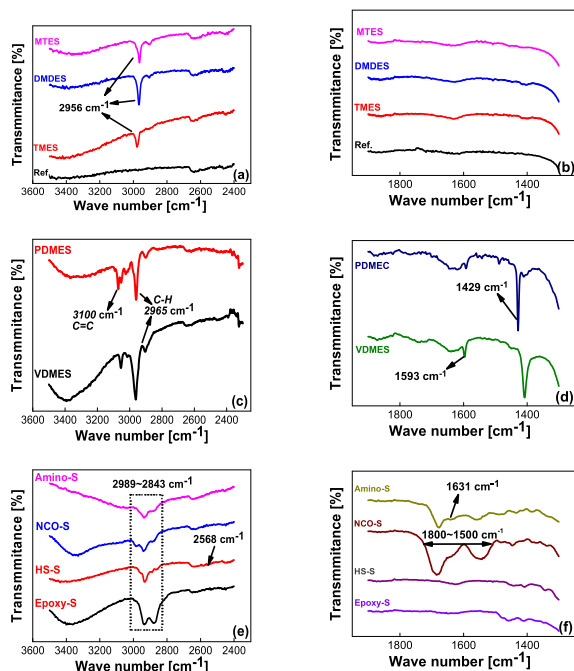
FIGURE 9. FTIR spectra of unmodified and modified silicas with the silanes belonging to Group I (a, b), Group II (c, d) and Group III (e, f).

The bands at 3100 cm^{-1} and 1429 cm^{-1} presented in Fig.9 (c) and (d) result from the aromatic ring of PMDES

[26, 27]. The presence of the vinyl group can be proven by the absorption band at 1593 cm^{-1} [26].

The bands at 2989~2843 cm^{-1} corresponding to the C-H [28] vibrations shown in Fig.9 (e) demonstrate, that all four polar silanes are grafted onto the silica surface. The intensive C-H stretching band in Fig.9 (e) indicates the presence of the epoxy silane on the silica surface due to the high number of CH_2 units in the chemical structure of this silane, although the bands from the epoxy ring group were not detected [29]. The broad band around 1631 cm^{-1} visible in Fig.9 (f) and assigned to N-H stretching belongs to the amine group of the amino silane [28]. Due to the sensitivity of the N=C=O group to water, it can be easily turned into a urethane group. Therefore, the bands at 1600~1500 cm^{-1} from the distortion oscillation of N-H and stretching oscillation of C-N, and the band at 1800-1600 cm^{-1} from stretching oscillation of C=O represent the presence of urethane, which proves the NCO-silane grafting onto the silica surface and its further reaction with water to form urethane groups.

It needs to be admitted that it is difficult to detect a S-H band at 2568 cm^{-1}, because it gives a very weak response in FTIR [28]. Nevertheless, all above results can prove that all the silanes were successfully grafted onto the silica surface through solvent-free modification.

### 3) TRANSMISSION ELECTRON MICROSCOPY (TEM) WITH ELEMENTAL MAPPING

To visualize the morphology of a silica surface with silane grafted onto it, TEM elemental mapping was carried out on the silica modified with amino-silane (Fig.10). It shows that the average size of the primary particles of the modified silica is around 20 nm, which is more or less as same size as untreated fumed silica particles. Elemental mapping was performed in order to identify the distribution of carbon (Fig.10 (b)) and silicon (Fig.10 (c)) on the silica surface after modification. Fig.10 (d) reveals the silane layer depicted in green with a smooth surface and a thickness of approximately 1 nm.

C. CHARACTERIZATION OF PP/POE OF NANOCOMPOSITES

1) DIFFERENTIAL SCANNING CALORIMETRY (DSC)

Fig.11 and Fig.12 represent the crystallization and melting behavior of all PP/POE nanocomposites, respectively. The crystallization parameters are shown in TABLE 6. It is obvious that there are two melting and crystallization peaks corresponding to the two polymer phases. In accordance with the previous results [30], the first peak at the lower temperature originates from the POE phase, in which the crystalline PE domains melt (or crystallize), while the second peak at higher temperature comes from the PP phase.

In general, the modified silica has a more pronounced effect on the crystallization behavior of both phases, PP and POE, than unmodified silica. The exothermic peak of the PP and POE phase is shifted to higher temperature values,
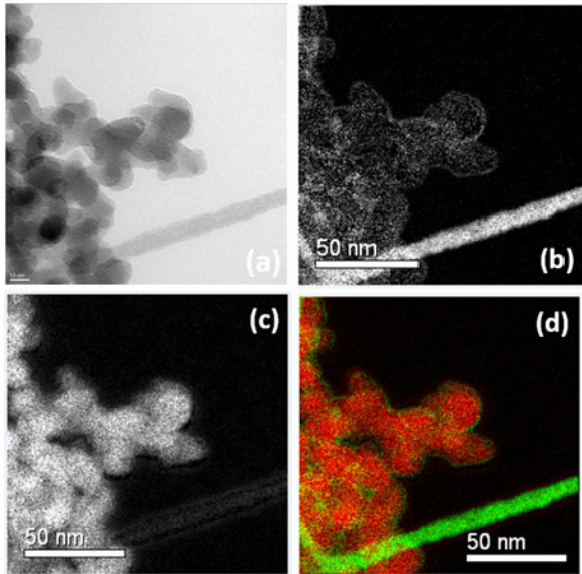
FIGURE 10. TEM elemental mapping image of silica modified with amino silane. (a: TEM image of modified silica; b: carbon mapping; c: silicon mapping; d: combined mapping images of carbon in green and silicone in red)).
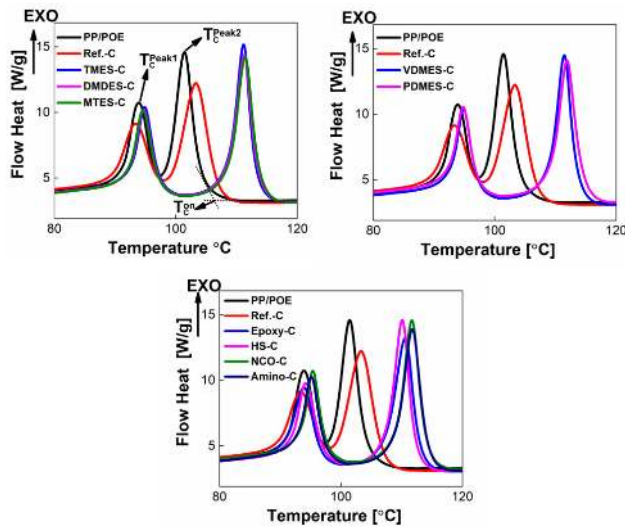
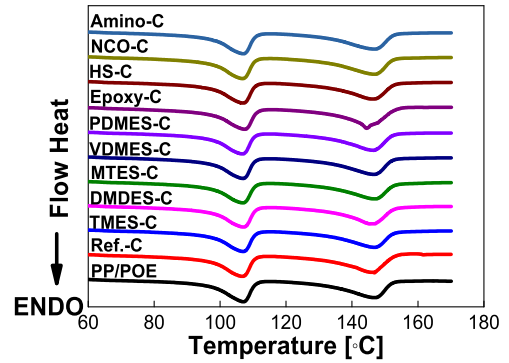**FIGURE 11.** DSC crystallization curves for PP/POE nanocomposites with unmodified silica (Ref.-C) and silica modified with the silanes described in Tables 2-4.

FIGURE 12. DSC melting curves for PP/POE nanocomposites.

suggesting a strong nucleating effect of the modified silicas [31, 32]. This also corresponds to literature, stating that silica can act as a heterogeneous nucleating agent because of the high specific surface area [33]. According to literature, the new silica/polymer interface reduces the nuclei size needed for crystal growth. This is due to the creation of an interface between the polymer crystal and the substrate, which might be less hindered than the formation of the corresponding free polymer morphology [34].

However, the nucleating effect is different in the separate PP and POE phases. There is a significant shift of the

crystallization onset temperature of approx. 10 °C with regard to the $T_C^{Peak\ 2}$ of the PP phase compared to a smaller shift of approx. 1 °C of $T_C^{Peak\ 1}$ of the POE phase: this indicates that the silica exhibits a more pronounced effect on the PP phase than on the POE phase. One of the reasons for it is the favored location of silica in the PP phase caused by the lower viscosity of the polymer compared to POE.

It is also worth noting that the silicas modified with the different types of silanes also exhibit different levels of impact on the crystallization behavior of the PP/POE composites. The silicas modified with unpolar silanes (TMES, DMDES, MTES, VDMES and PDMES) exhibit a consistent shift on the exothermic peak shown in TABLE 6 and marked in red font, while the silicas modified with the polar silanes (HS-silane, epoxy-silane, NCO-silane and amino-silane) give various values of temperature shift. This is most likely due to the differences in silica/polymer compatibility. The silicas modified with unpolar silanes exhibit better compatibility with the polymer blend than the silicas modified with polar silanes. Moreover, the PP phase crystallization temperature also varies with polarity of the silane and their chemical nature.

Crystallinity was additionally calculated from DSC melting curves based on Equation (3):

$$X_C = \frac{\Delta H_C}{w \Delta H_{100}} 100 \qquad (3)$$

where,

ΔH_C = heat of crystallization (J/g)

W = weight percent of the polymer.

ΔH_{100} is the heat of crystallization of the hypothetical 100% crystalline polymer. PP and POE blends are used in our study; POE is a copolymer containing PE as crystalline phase. In this equation, the ΔH_{100} value of 209 J/g for PP [35] and 293 J/g for PE [36] were used. The results are presented in Table 6. Compared to the neat PP/POE, the crystallization energy of the PP/POE nanocomposites are rather similar, indicating that the degree of crystallinity of PP/POE was not changed.

The melting curves of all samples are shown in Fig.12. Compared to the crystallization temperature, there is no

TABLE 6. DSC crystallization results for PP/POE nanocomposites.

Sample	T_C^{peak1} (°C)	T_C^{peak2} (°C)	T_C^{on} (°C)	ΔH_C (J/g)	X_C (%)
PP/POE	93.8	101.4	104.1	71.1	28.5
Ref-C	93.3	103.3	107.0	70.6	28.3
TMES-C	94.9	111.1	113.2	69.9	28.0
DMDES-C	94.7	111.2	113.5	69.8	27.9
MTES-C	94.6	111.4	113.8	69.5	27.8
VDMES-C	94.9	111.4	113.7	69.2	27.7
PDMES-C	94.7	111.8	114.5	70.3	28.2
Epoxy-C	93.9	110.6	113.1	68.9	27.6
HS-C	94.0	110.0	112.3	69.2	27.7
NCO-C	95.4	111.7	114.3	68.8	27.6
Amino-C	95.1	111.7	114.1	70.2	28.1

T_C^{peak1} : crystallization peak temperature of the POE phase;
T_C^{peak2} : crystallization peak temperature of the PP phase;
$T_C on$: onset of crystallization peak of the PP phase;
ΔH_C : total heat during the crystallization process;
X_C : calculated crystallinity of PP/POE nanocomposites.
Marked in red exothermic peak temperature of PP/POE filled with unpolar silica.
Marked in blue: exothermic peak temperature of PP/POE filled with the polar silica.

significant difference of melting temperature between neat PP/POE and silica-filled PP/POE composites; this effect was also reported in the literature [37].

2) X-RAY DIFFRACTION (XRD)

In order to gain a better understanding of the influence of the modified silicas on the crystallization behavior of the PP/POE nanocomposites, XRD measurements were conducted on all the samples. The results are shown in Fig.13. Three different crystal phases (α and β crystals of the PP phase and orthorhombic crystals from the PE phase) are detected, as have been reported in previous work [30]. It is important to notice that no obvious increase of the β crystal content in the silica filled PP/POE composites was recorded (both untreated and treated silicas). These results are similar to our previous findings, while it is different from results reported in literature: nanofillers to act as nucleating agents increasing the amount of β crystals under favorable crystallization conditions, [33]. Moreover, the degree of overall crystallinity and the PP phase crystallinity were calculated by dividing the total area of the crystalline peaks by the cooresponding area of all peaks; and the results are shown in TABLE 7. There is no significant difference in the crystalline phase content for any of the nanocomposites, which is in line with the DSC
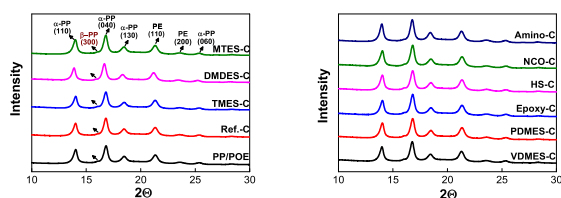

FIGURE 13. XRD curves of all PP/POE nanocomposites.

TABLE 7. Calculated crystallinity based on XRD curves of all PP/POE nanocomposites.

Composites	Overall Crystallinity / %	PP phase Crystallinity / %
PP/POE	44.6	32.3
Ref-C	43.7	31.6
TMES-C	43.2	31.2
DMDES-C	44.1	31.9
MTES-C	45.7	33.0
VDMES-C	44.6	32.2
PDMES-C	44.2	31.9
Epoxy-C	44.4	32.1
HS-C	44.0	31.8
NCO-C	45.1	32.6
Amino-C	47.3	34.2

results. In summary, 1% of silica does not significantly affect the degree of crystallinity; however, it influences strongly the crystallization behavior of PP/POE composites with an emphasis on the PP phase, where it acts as a strong nucleating agent.

3) SCANNING ELECTRON MICROSCOPY (SEM)

The morphology of the PP/POE nanocomposites was evaluated by SEM. The samples were broken after cooling in liquid N_2 (at a temperature below the Tg's of the polymers) and analyzed without surface coating. Two images of each sample with magnification of 50K and 20K are shown in Fig. 14, 15 and 16.
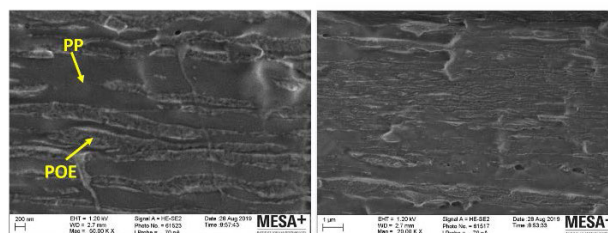
FIGURE 14. SEM image of unfilled PP/POE composites (Left 50K and Right 20K).

The SEM pictures show clearly that there are two phases evenly mixed together layer by layer in the unfilled PP/POE composites in Fig.14 and in the silica filled PP/POE nanocomposites in Fig.15 and 16. One of the phase has a smooth surface, whereas the other one appears more rough/granular. Moreover, it is interesting that all the silicas, including the reference silica and the modified silicas, are by preference located in one of the phases, the smooth phase, which is coherent with the DSC results. From the DSC results, it could be concluded that the silica has a more pronounced influence on the PP phase by means of the crystallization peak shift. Therefore, we can deduct that the
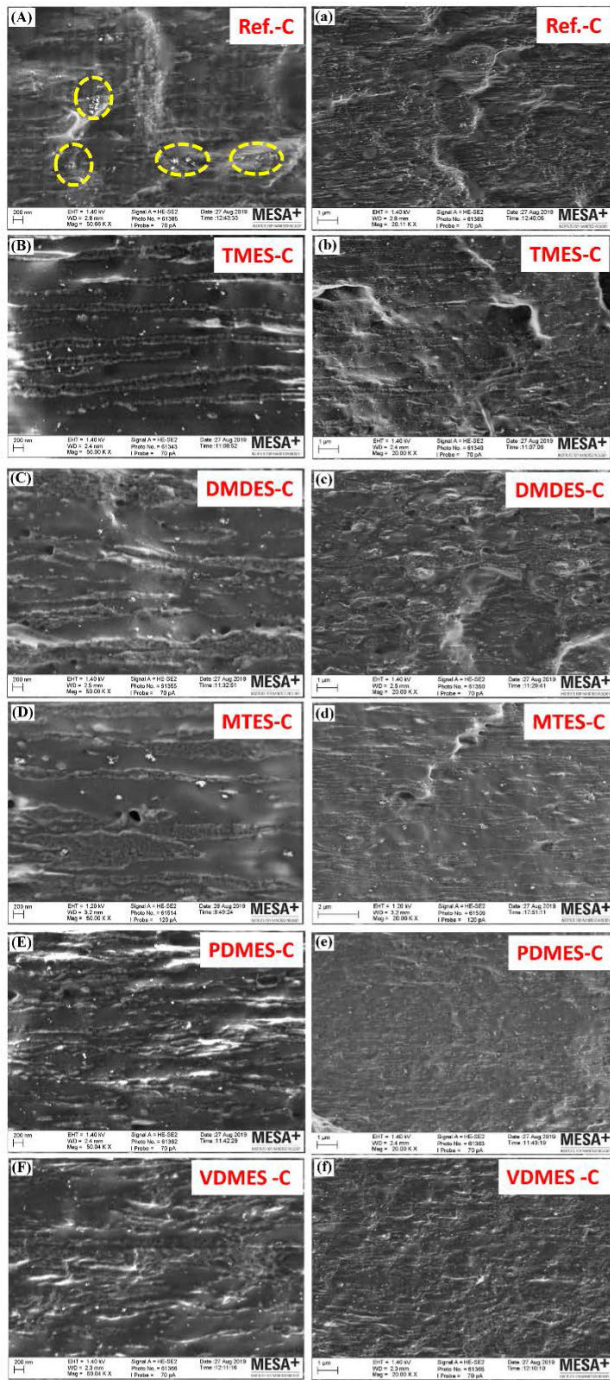
FIGURE 15. SEM images of PP/POE composites filled with the reference silica and modified hydrophobic silicas ((Left 50K and Right 20K)).

FIGURE 16. SEM images of PP/POE composites filled with the reference silica and modified hydrophilic silicas ((Left 50K and Right 20K)).

smooth phase shown in the SEM images is the PP phase, while the rough phase is POE. The preferential location of the silica in the PP phase can be explained by the lower viscosity of this phase. PP is a thermoplastic material, while POE exhibits elastomeric properties and therefore a higher viscosity.

Regarding the dispersion of silica, Fig.15 (A and a) shows some agglomerates in the reference silica filled PP/POE composites, and the silica is not evenly distributed in the polymer

matrix. Whereas the silicas modified with the unpolar silanes (TMES, DMDES, MTES, VDMES or PDMES) exhibit better dispersion and distribution within the polymer matrix, which is shown in Fig.15 (B, C, D, E, F and b, c, d, e, f). This is due to a higher compatibility between the modified hydrophobic silicas and the PP/POE polymer matrix.

In Fig.16, all silicas modified with hydrophilic silanes are shown (HS-silane, epoxy-silane, NCO-silane or amino-silane). As all modified silicas shown in Fig.16 still retain their hydrophilic nature, they are less compatible with the unpolar polymer matrix. Consequently, these silicas are more likely to agglomerate and form clusters, which are strongly connected by polar-polar interactions, and therefore exhibit a lower degree of dispersion and distribution in the PP/POE polymer matrix.

4) THERMALLY STIMULATED DEPOLARIZATION CURRENT (TSDC)

To investigate the influence of different surface-modified silicas on the charge trapping properties in PP/POE nanocomposites, TSDC measurements were performed. The measured TSDC spectra are shown in Fig.17 A, B and C. The current formed by the relaxation of trapped charges during the
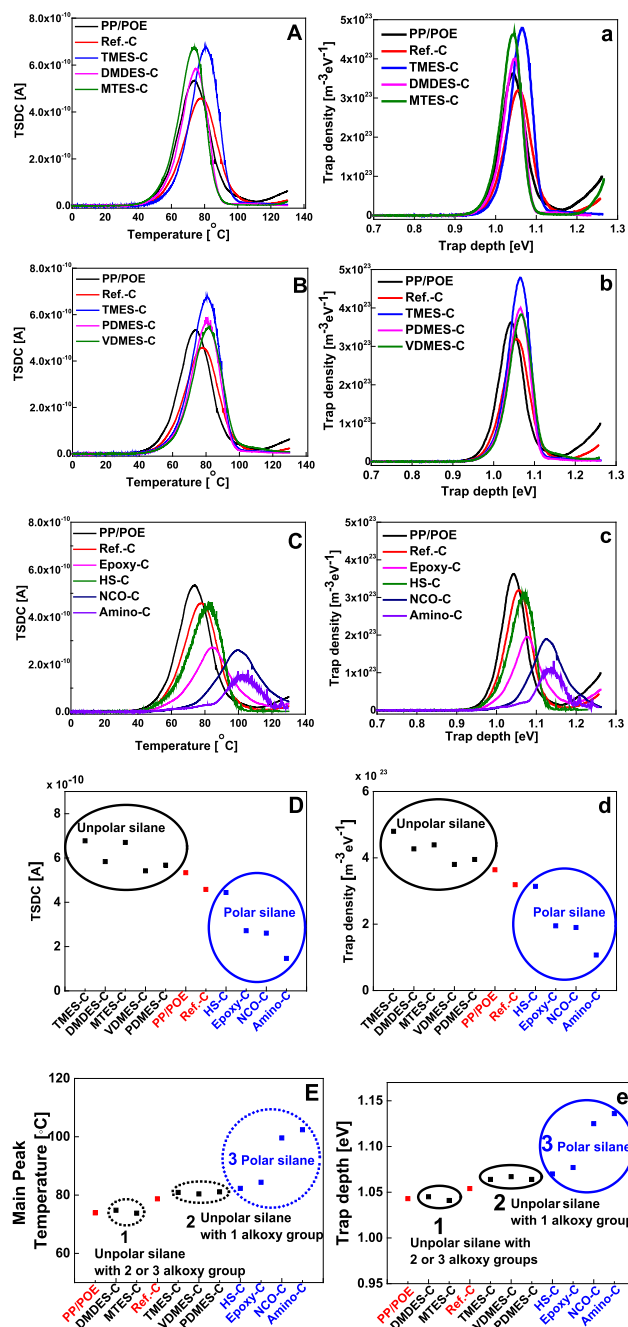
FIGURE 17. TSDC results of all composites and the calculated trap density and depth. Region 1 is the main peak temperature (left) and the trap depth of the PP/POE composites filled with the silica modified with the unpolar silane with 2 or 3 alkoxy groups. Region 2 is the main peak temperature (left) and the trap depth of the PP/POE composites filled with the silica modified with the unpolar silane with 1 alkoxy group. Region 3 is the main peak temperature (left) and the trap depth of the PP/POE composites filled with the silica modified with the polar silane.

thermally stimulated depolarization process is related to the charge trap distribution in the nanocomposites. In principle, the TSDC current intensity is associated with the trap density, and the TSDC temperature is related to the trap depth. The calculated trap depth vs. density distributions, obtained from the TSDC spectra by using a numerical method presented in [38] are shown in Fig.17 a, b and c.

As shown in the Fig.17, the silicas treated with different silanes tailor the charge trapping properties of the PP/POE composites. With increasing temperature the TSDC current starts to rise from 30 °C onwards, corresponding to the onset of charge relaxation. The TSDC measurement range for all the PP/POE samples is the same, from 50 °C to 130 °C, limited by the melting temperature of the PP phase. The TSDC peak intensity (apparent trap density) and peak temperature (trap depth) are changing and varying for the PP/POE nanocomposites filled with different modified silica.

It is interesting to notice that the TSDC peak intensity (apparent trap density) is higher for the PP/POE nanocomposites filled with the silicas modified by unpolar silanes such as TMES, DMDES, MTES, VDMES and PDMES than for the silicas modified by polar silanes (HS-silane, epoxy-silane, NCO-silane, amino-silane), as shown in Fig.17 D. Since there is no significant difference in the degree of crystallinity for the silica filled PP/POE nanocomposites based on the DSC and XRD results, the differences in TSDC spectra are attributed to new trap sites arising from the chemical nature of the surface modification. These traps (associated with the silica surface functionalization) are then dispersed along with the silica throughout the matrix. In addition, the interface between a silica and polymer matrix plays an important role in the charge trapping properties. It has been reported that adding nanoparticles can introduce a large interfacial area [6] resulting in higher amount of traps formed in nanodielectrics [39].

In our study, we applied 9 silanes to be grafted onto silica surface, which lead to different compatibilities between the modified silicas and the polymer matrix. The silicas modified with unpolar silanes (TMES, DMDES, MTES, VDMES or PDMES) exhibit better compatibility with the PP/POE matrix. This resulted in better dispersion of the unpolar modified silicas in the PP/POE matrix and implied a larger interfacial area (Fig.18 left) between silica and PP/POE matrix, which is consistent with the SEM results presented in Figure 15. Consequently, a higher peak intensity (trap density) is measured as shown in Fig.17 A, a and 17 B, b. On the contrary, the unmodified silica and the silica modified with polar silanes (HS-silane, epoxy-silane, NCO-silane, amino-silane) still tend to agglomerate and have a lower compatibility towards the PP/POE matrix, which is also seen in the SEM images in Fig.16. As a result, compared to the unpolar silica less interface (Fig.18 right) is formed. This resulted in
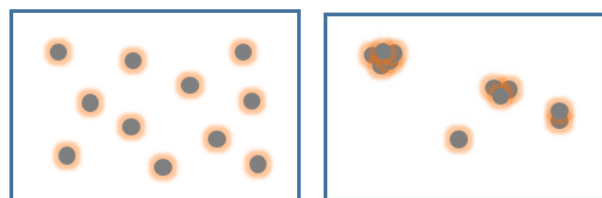
FIGURE 18. Schemes of the interface area between silica and matrix. (Left: Unpolar silica, good dispersion; right: polar silica forming clusters.

a lower TSDC peak intensity and apparent trap density as shown in Fig.17 C and c.

The differences observed in TSDC peak intensity (apparent trap density) of the nanocomposites may also be linked to differences in their trap depth and charge mobility. During the isothermal polarization stage, the charges are injected and trapped into the samples, with the temperature- and field-dependent charge mobility and trapping phenomena dictating the total amount of accumulated charge. Subsequently, during the thermally stimulated depolarization stage, the previously accumulated space charge in the sample is relaxed (detrapped). Thus, the TSDC peak intensity is in principle related to the amount of injected charge (neglecting e.g. charge recombination inside the specimen). With increasing trap depth, the build-up of deeply trapped homocharge layer near the electrode-specimen interface reduces further charge injection, and thus higher temperature or electric field would be required during the polarization step to inject more charge. Therefore, under the same polarization temperature and electric field, less charge is accumulated in the sample with a higher trap depth, with this also resulting in lower TSDC current intensity and apparent trap density, which is line with our observations.

It is important to notice that the trap depth also varies for the composites containing differently modified silicas (Fig.17 e). It is obvious from Fig.17 E that there is a large peak temperature shift (approx. 10 ~30 °C) to a higher level for the nanocomposites filled with the polar silane modified silicas. These polar silanes contain hetero-atoms (S, O or N) imposing the polar character of the functional moieties to the silica surface. Therefore, the silicas modified with polar silanes introduce deeper traps into the nanocomposites. This phenomenon is also described in literature, where studies or models indicate that polar groups or hetero-atoms of electronegativity higher than the one of carbon can introduce deep traps [11], [40]–[42]. It is worth to note that the most pronounced one is the silica modified with NCO and amino silanes, which both contain a nitrogen atom.

Regarding to the silicas modified with the unpolar silanes in Fig.17 A and B, the results are also very interesting. Although there is no significant shift of the peak temperature compared with the one modified with polar silane in Fig.17 C, a small variation of approximately 5 °C is measured, see Fig.17 E. In order to explain, why silica modified with unpolar silanes give different results concerning the trap level, a hypothesis is depicted in Fig.19. As discussed above, there is an organic layer on silica surface after the modification. The efficiency of the silane shielding of the silica surface is dependent on the number of alkoxy groups in the silane molecule as shown in Fig.19. Therefore, the surface properties of silica are altered via the silane agents containing various numbers of alkoxy groups. Consequently, the interface between silica and the polymer matrix is also affected.

Due to condensation of silanes, the silica modified with the silane containing two or three alkoxy groups shield efficiently the silica surface based the calculated the amount of grafed
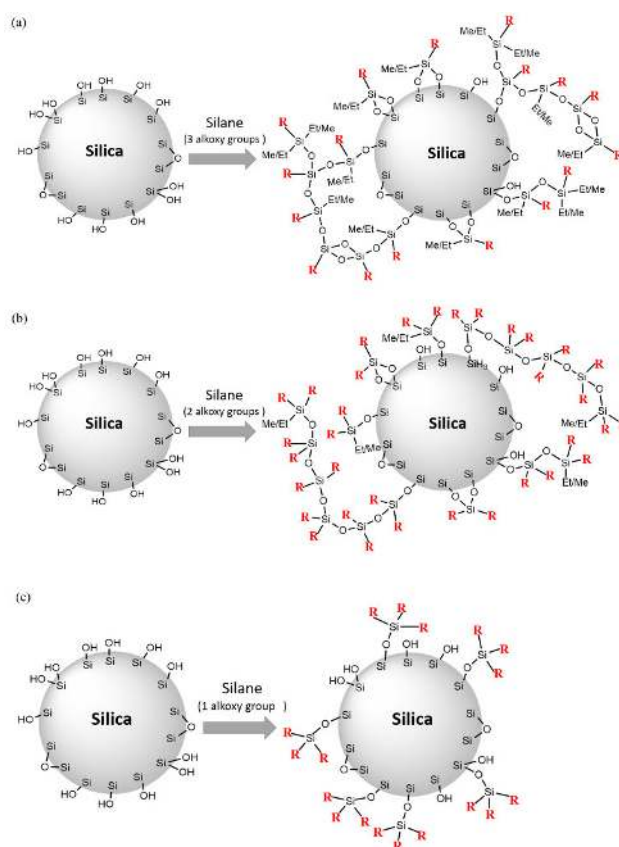
FIGURE 19. Schemes of silica surface modification and shielding effect by silanes having different number of alkoxy groups.

silane on silica surface in Fig.8 right. As a result, all unreacted silanol or siloxane groups are covered by silane molecules as shown in Fig.19 (a) and (b). Therefore, the silicas modified with DMDES or MTES have their surface covered by a hydrocarbon layer, which exhibits a similar physicochemical character as the polymer matrix. As a result shown in Region 1 in Fig.17 E, the temperature of the main TSDC peak of the composites filled with DMDES or MTES modified silicas is more or less the same as for the unfilled PP/POE matrix. In conclusion, there is no new deep trap introduced due to a similar energy state of hydrocarbons at the interface between the modified silicas and polymer matrix.

However, if the silica was modified with a silane containing only one alkoxy group, there are still unreacted silanol or siloxane groups exposed on the silica surface (Fig.19 (c)). This inefficient shielding will influence the final interface properties between the silica and a polymer matrix [40]. As a result, the silica modified with TMES, VDMES or PDMES have still unreacted silanol or siloxane group exposed to the Polymer matrix. There are new deeper traps introduced by the O- or Si-atoms on the silica surface, which are located in the interface between silica and the polymer matrix, due to a different energy state of atoms (O, Si, C, H). Consequently, the maximum of the main TSDC peak temperature is shifted to a higher temperature as shown in Region 2 in Fig.17 E.

In order to further analyze the TSDC results, the amount of charge injected during the isothermal polarization and the amount of charge released from the samples during the TSDC measurement were calculated by integrating the current versus time curves during polarization and depolarization (Fig.20 left). In principle, for unpolar polymers, when the temperature is above the glass transition temperature, the TSDC current is mostly due to the space charge relaxation. This relaxation is influenced by the chemical and structural characteristics [43].
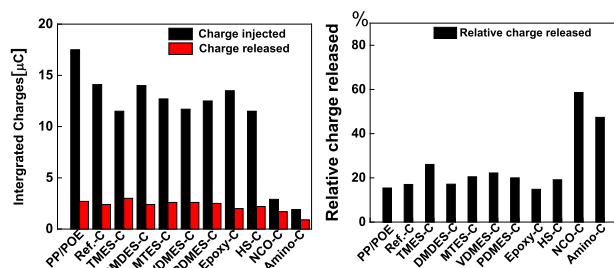

FIGURE 20. Calculated injected charge and relative released charge during TSDC.

In comparison with the neat PP/POE matrix, the amount of charges injected into the samples during the polarization decreased for the samples filled with the reference silica and silane modified silicas, indicating lower charge mobility for all these nanocomposites. It is also noticeable that a much lower amount of charges was injected into the NCO silane and amino silane modified silica filled composites than into the composites containing silicas modified with other silanes.

The relative amount of released charges was also calculated and shown in Fig.20 right. In general, this value increased for all the nanocomposites containing the reference silica or modified silicas compared to the unfilled PP/POE matrix. However, there is a more significant rise when incorporating the silica modified by NCO and amino silane. This means that less charges are permanently trapped or dissipated in the NCO or amino silane modified-silica filled composites. In other words, incorporation of the NCO or amino silane modified silicas can significantly suppress the space charge accumulation effect of the PP/POE composites. This might be due to the polar NCO or amino group, which can form large dipoles and introduce deeper traps [41]. The trap depth of these materials is large enough to block the movement of the charge carrier, leading to suppression of space charge formation [44].

IV. CONCLUSIONS

Based on the investigations performed and presented in this paper, the following conclusions can be drawn:

- A new solvent-free silane-silica modification method was developed. A catalyst (acid or base) successfully accelerates the silica surface modification. The efficiency of this method was supported by TGA, FTIR, XPS and TEM elemental mapping measurements.

- Based on the TGA results, the modification of the silica surface assisted by an acid catalyst is more stable than the one achieved by a base catalyst.
- Successful silica modification was achieved using 9 different silanes, which was proven by TGA and FTIR results.
- When blended with a PP/POE matrix, the silicas increased the onset of the crystallization temperature due to the nucleation effect. This effect was most prominent in the PP phase, where the silica particles were preferentially located. In terms of degree of crystallinity, DSC and XRD results both confirmed that there is barely any influence of adding these silicas.
- Based on SEM images, silica modified with unpolar silanes were easier to disperse in a PP/POE polymer matrix, while the ones modified with polar silanes agglomerated in the polymer matrix.
- Based on the TSDC results, the efficiency of covering the silica surface depends on the number of alkoxy groups in the silane. This influences the charge trapping properties noticeably.
- TSDC results have shown as well, that the PP/POE nanocomposites filled with an unpolar silane increased the charge trap density, while the ones filled with a polar silica increased the charge trap depth.
- Silica modified with the polar silane containing nitrogen atoms showed less injected charges, which might be an indication of suppressing the space charge accumulation by introducing nitrogen-rich polar functional groups.

REFERENCES

[1] Y. Gao, J. Li, Y. Yuan, S. Huang, and B. Du, "Trap distribution and dielectric breakdown of isotactic Polypropylene/Propylene based elastomer with improved flexibility for DC cable insulation," *IEEE Access*, vol. 6, pp. 58645–58661, 2018.

[2] I. Rytoluoto, M. Ritamäki, K. Lahti, M. Paajanen, M. Karttunen, G. C. Montanari, P. Seri, and H. Naderiallaf, "Compounding, structure and dielectric properties of silica-BOPP nanocomposite films," in *Proc. IEEE 2nd Int. Conf. Dielectr. (ICD)*, Hong Kong, Jul. 2018, pp. 1–4.

[3] E. Helal, C. Pottier, E. David, M. Fréchette, and N. R. Demarquette, "Polyethylene/thermoplastic elastomer/Zinc oxide nanocomposites for high voltage insulation applications: Dielectric, mechanical and rheological behavior," *Eur. Polym. J.*, vol. 100, pp. 258–269, Mar. 2018.

[4] A. M. Pourrahimi, R. T. Olsson, and M. S. Hedenqvist, "The role of interfaces in polyethylene/metal-oxide nanocomposites for ultrahigh-voltage insulating materials," *Adv. Mater.*, vol. 30, no. 4, 2018, Art. no. 1703624.

[5] L. K. H. Pallon, A. T. Hoang, A. M. Pourrahimi, M. S. Hedenqvist, F. Nilsson, S. Gubanski, U. W. Gedde, and R. T. Olsson, "The impact of MgO nanoparticle interface in ultra-insulating polyethylene nanocomposites for high voltage DC cables," *J. Mater. Chem. A*, vol. 4, no. 22, pp. 8590–8601, 2016.

[6] M. Roy, J. K. Nelson, R. K. MacCrone, L. S. Schadler, C. W. Reed, and R. Keefe, "Polymer nanocomposite dielectrics–The role of the interface," *IEEE Trans. Dielectr. Electr. Insul.*, vol. 12, no. 4, pp. 629–643, Aug. 2005.

[7] D. Liu, A. T. Hoang, A. M. Pourrahimi, L. K. H. Pallon, F. Nilsson, S. M. Gubanski, R. T. Olsson, M. S. Hedenqvist, and U. W. Gedde, "Influence of nanoparticle surface coating on electrical conductivity of LDPE/Al2O3 nanocomposites for HVDC cable insulations," *IEEE Trans. Dielectrics Electr. Insul.*, vol. 24, no. 3, pp. 1396–1404, Jun. 2017.

[8] D. Ma, T. A. Hugener, R. W. Siegel, A. Christerson, E. Märtensson, C. Önneby, and L. S. Schadler, "Influence of nanoparticle surface modification on the electrical behaviour of polyethylene nanocomposites," *Nanotechnology*, vol. 16, no. 6, pp. 724–731, Jun. 2005.

[9] X. Huang, P. Jiang, and Y. Yin, "Nanoparticle surface modification induced space charge suppression in linear low density polyethylene," *Appl. Phys. Lett.*, vol. 95, no. 24, Dec. 2009, Art. no. 242905.

[10] M. Bell, T. Krentz, J. K. Nelson, L. Schadler, K. Wu, C. Breneman, S. Zhao, H. Hillborg, and B. Benicewicz, "Investigation of dielectric breakdown in silica-epoxy nanocomposites using designed interfaces," *J. Colloid Interface Sci.*, vol. 495, pp. 130–139, 2017.

[11] S. Li, D. Min, W. Wang, and G. Chen, "Linking traps to dielectric breakdown through charge dynamics for polymer nanocomposites," *IEEE Trans. Dielectr. Electr. Insul.*, vol. 23, no. 5, pp. 2777–2785, Oct. 2016.

[12] S. Li, G. Yin, G. Chen, J. Li, S. Bai, L. Zhong, Y. Zhang, and Q. Lei, "Short-term breakdown and long-term failure in nanodielectrics: A review," *IEEE Trans. Dielectr. Electr. Insul.*, vol. 17, no. 5, pp. 1523–1535, Oct. 2010.

[13] A. Mahtabani, X. He, I. Rytöluoto, K. Lahti, M. Paajanen, E. Saarimaki, R. Anyszka, W. Dierkes, and A. Blume, "Effect of silica modification on charge trapping behavior of PP blend/silica nanocomposites," in *Proc. 2nd Int. Conf. Electr. Mater. Power Equip. (ICEMPE)*, Beijing, China, Apr. 2019, pp. 241–245.

[14] X. He, A. Mahtabani, I. Rytöluoto, E. Saarimaki, K. Lahti, M. Paajanen, R. Anyszka, W. Dierkes, and A. Blume, "Surface modification of fumed silica by dry silanization for PP-based dielectric nanocomposites," in *Proc. 2nd Int. Conf. Electr. Mater. Power Equip. (ICEMPE)*, Beijing, China, Apr. 2019, pp. 254–259.

[15] A. Mathabani, I. Rytöluoto, X. He, E. Saarimäki, K. Lahti, M. Paajanen, R. Anyszka, W. Dierkes, and A. Blume, "Solution modified fumed silica and its effect on charge trapping behavior of PP/POE/silica nanodielectrics," in *Proc. Nordic Insul. Symp.*, Helsinki, Finland, vol. 26, 2019, pp. 129–133.

[16] A. C. Borges-Muñoz, D. P. Miller, E. Zurek, and L. A. Colón, "Silanization of superficially porous silica particles with P-aminophenyltrimethoxysilane," *Microchem. J.*, vol. 147, pp. 263–268, Jun. 2019.

[17] J. S. Sonn, J. Y. Lee, S. H. Jo, I.-H. Yoon, C.-H. Jung, and J. C. Lim, "Effect of surface modification of silica nanoparticles by silane coupling agent on decontamination foam stability," *Ann. Nucl. Energy*, vol. 114, pp. 11–18, Apr. 2018.

[18] H. Hemmatpour, V. Haddadi-Asl, and H. Roghani-Mamaqani, "Synthesis of pH-sensitive poly (N,N-dimethylaminoethyl methacrylate)-grafted halloysite nanotubes for adsorption and controlled release of DPH and DS drugs," *Polymer*, vol. 65, pp. 143–153, May 2015.

[19] Y. W. Ngeow, A. V. Chapman, J. Y. Y. Heng, D. R. Williams, S. Mathys, and C. D. Hull, "Characterization of silica modified with silanes by using thermogravimetric analysis combined with infrared detection," *Rubber Chem. Technol.*, vol. 92, no. 2, pp. 237–262, Apr. 2019.

[20] L. A. S. A. Prado, M. Sriyai, M. Ghislandi, A. Barros-Timmons, and K. Schulte, "Surface modification of alumina nanoparticles with silane coupling agents," *J. Brazilian Chem. Soc.*, vol. 21, no. 12, pp. 2238–2245, 2010.

[21] J. D. Rusmirović, T. Radoman, E. S. Däunuzović, J. V. Däunuzović, J. Markovski, P. Spasojević and A. D. Marinković, "Effect of the modified silica nanofiller on the mechanical properties of unsaturated polyester resins based on recycled polyethylene terephthalate," *Polym. Compos.*, vol. 38, no. 3, pp. 538–554, Mar. 2017.

[22] Z. Tang, J. Huang, X. Wu, B. Guo, L. Zhang, and F. Liu, "Interface engineering toward promoting silanization by ionic liquid for high-performance rubber/silica composites," *Ind. Eng. Chem. Res.*, vol. 54, no. 43, pp. 10747–10756, Nov. 2015.

[23] Y. Shin, D. Lee, K. Lee, K. H. Ahn, and B. Kim, "Surface properties of silica nanoparticles modified with polymers for polymer nanocomposite applications," *J. Ind. Eng. Chem.*, vol. 14, no. 4, pp. 515–519, 2008.

[24] W. He, D. Wu, J. Li, K. Zhang, Y. Xiang, L. Long, S. Qin, J. Yu, and Q. Zhang, "Surface modification of colloidal silica nanoparticles: Controlling the size and grafting process," *Bull. Korean Chem. Soc.*, vol. 34, no. 9, pp. 2747–2752, Sep. 2013.

[25] B. Qiao, T.-J. Wang, H. Gao, and Y. Jin, "High density silanization of nano-silica particles using γ-aminopropyltriethoxysilane (APTES)," *Appl. Surf. Sci.*, vol. 351, pp. 646–654, Oct. 2015.

[26] X. Yang, Q. Shao, L. Yang, X. Zhu, X. Hua, Q. Zheng, G. Song, and G. Lai, "Preparation and performance of high refractive index silicone resin-type materials for the packaging of light-emitting diodes," *J. Appl. Polym. Sci.*, vol. 127, no. 3, pp. 1717–1724, Feb. 2013.

[27] N. A. Negm, G. H. Sayed, F. Z. Yehia, O. I. Habib, and E. A. Mohamed, "Biodiesel production from one-step heterogeneous catalyzed process of castor oil and jatropha oil using novel sulphonated phenyl silane montmorillonite catalyst," *J. Mol. Liquids*, vol. 234, pp. 157–163, May 2017.

[28] F. Zucchi, A. Frignani, V. Grassi, G. Trabanelli, and M. DalColle, "The formation of a protective layer of 3-mercapto-propyl-trimethoxy-silane on copper," *Corrosion Sci.*, vol. 49, no. 3, pp. 1570–1583, Mar. 2007.

[29] J. C. Hoepfner and S. H. Pezzin, "Functionalization of carbon nanotubes with (3-glycidyloxypropyl)-trimethoxysilane: Effect of wrapping on epoxy matrix nanocomposites," *J. Appl. Polym. Sci.*, vol. 133, no. 47, p. 44245, Dec. 2016.

[30] X. He, I. Rytöluoto, R. Anyszka, A. Mahtabani, E. Saarimäki, K. Lahti, M. Paajanen, W. Dierkes, and A. Blume, "Surface modification of fumed silica by plasma polymerization of acetylene for PP/POE blends dielectric nanocomposites," *Polymers*, vol. 11, no. 12, p. 1957, 2019.

[31] B. Dang, J. He, J. Hu, and Y. Zhou, "Tailored sPP/silica nanocomposite for ecofriendly insulation of extruded HVDC cable," *J. Nanomater.*, vol. 2015, Dec. 2015, Art. no. 686248.

[32] J. Qian, P. He, and K. Nie, "Nonisothermal crystallization of PP/nano-SiO₂ composites," *J. Appl. Polym. Sci.*, vol. 91, no. 2, pp. 1013–1019, Jan. 2004.

[33] S. Borysiak, Å. Klapiszewski, K. Bula, and T. Jesionowski, "Nucleation ability of advanced functional silica/lignin hybrid fillers in polypropylene composites," *J. Thermal Anal. Calorimetry*, vol. 126, no. 1, pp. 251–262, Oct. 2016.

[34] M. Mucha and Z. Królikowski, "Application of dsc to study crystallization kinetics of polypropylene containing fillers," *J. Thermal Anal. Calorimetry*, vol. 74, no. 2, pp. 549–557, 2003.

[35] Y. Zare and H. Garmabi, "Nonisothermal crystallization and melting behavior of PP/nanoclay/CaCO3 ternary nanocomposite," *J. Appl. Polym. Sci.*, vol. 124, no. 2, pp. 1225–1233, Apr. 2012.

[36] F. M. Mirabella and A. Bafna, "Determination of the crystallinity of polyethylene/α-olefin copolymers by thermal analysis: Relationship of the heat of fusion of 100% polyethylene crystal and the density," *J. Polym. Sci. B, Polym. Phys.*, vol. 40, no. 15, pp. 1637–1643, Aug. 2002.

[37] L. Huang, R. Zhan, and Y. Lu, "Mechanical properties and crystallization behavior of Polypropylene/Nano-SiO2 composites," *J. Reinforced Plastics Compos.*, vol. 25, no. 9, pp. 1001–1012, Jun. 2006.

[38] F. Tian, W. Bu, L. Shi, C. Yang, Y. Wang, and Q. Lei, "Theory of modified thermally stimulated current and direct determination of trap level distribution," *J. Electrostatics*, vol. 69, no. 1, pp. 7–10, Feb. 2011.

[39] B. X. Du, H. Xu, J. Li, and Z. Li, "Space charge behaviors of PP/POE/ZnO nanocomposites for HVDC cables," *IEEE Trans. Dielectr. Electr. Insul.*, vol. 23, no. 5, pp. 3165–3174, Oct. 2016.

[40] B. Du, J. Su, M. Tian, T. Han, and J. Li, "Understanding trap effects on electrical treeing phenomena in EPDM/POSS composites," *Sci. Rep.*, vol. 8, no. 1, Dec. 2018, Art. no. 8481.

[41] M. Roy, J. K. Nelson, R. K. MacCrone, and L. S. Schadler, "Candidate mechanisms controlling the electrical characteristics of silica/XLPE nanodielectrics," *J. Mater. Sci.*, vol. 42, no. 11, pp. 3789–3799, Jun. 2007.

[42] G. Teyssedre and C. Laurent, "Charge transport modeling in insulating polymers: From molecular to macroscopic scale," *IEEE Trans. Dielectrics Electr. Insul.*, vol. 12, no. 5, pp. 857–875, Oct. 2005.

[43] V. M. Gun'ko, V. I. Zarko, E. V. Goncharuk, L. S. Andriyko, V. V. Turov, Y. M. Nychiporuk, R. Leboda, J. Skubiszewska-Zieba, A. L. Gabchak, V. D. Osovskii, Y. G. Ptushinskii, G. R. Yurchenko, O. A. Mishchuk, P. P. Gorbik, P. Pissis, and J. P. Blitz, "TSDC spectroscopy of relaxational and interfacial phenomena," *Adv. Colloid Interface Sci.*, vol. 131, nos. 1–2, pp. 1–89, Feb. 2007.

[44] T. Takada, Y. Hayase, Y. Tanaka, and T. Okamoto, "Space charge trapping in electrical potential well caused by permanent and induced dipoles for LDPE/MgO nanocomposite," *IEEE Trans. Dielectr. Electr. Insul.*, vol. 15, no. 1, pp. 152–160, Oct. 2008.

XIAOZHEN HE (Member, IEEE) was born in Yantai, Shandong, China, in 1990. She received the M.Sc. degree in polymer chemistry and physics from the Qingdao University of Science and Technology, China, in 2017, and the Ph.D. degree from the Elastomer Technology and Engineering Group, University of Twente, Enschede, The Netherlands, in 2017.

She is currently working on the EU project GRIDABLE. The aim of this project is to develop novel dielectric thermoplastic polymer composite materials for HVDC cable and dc capacitors application. In this project, she is responsible for the nanofiller surface modification via solvent free method and plasma technology. Her research interests include HVDC cable insulation material, nanocomposites, nanofiller surface engineering, thermoplastic, rubber, and plasma technology.

AMIRHOSSEIN MAHTABANI (Member, IEEE) received the B.Sc. degree in polymer engineering from the University of Tehran, Iran, in 2013, and the M.Sc. degree in polymer engineering from Tarbiat Modares University, Iran, in 2015. He is currently pursuing the Ph.D. degree with the Chair of the Elastomer Technology and Engineering, University of Twente. His main research interests involve nanoparticle modification, nanocomposite development, interface engineering, and fabrication of nanostructured surfaces.

EETTA SAARIMÄKI received the M.Sc. (Tech.) degree in plastics technology from the Tampere University of Technology, Tampere, Finland, in 1993. She has been working at VTT Technical Research Centre of Finland Ltd., since 1994, where she is currently working as a Senior Scientist. Her research interests include plastic processing technologies (especially extrusion, compounding, and orientation), electromechanical films, plastic nanocomposites, functional polymer composites, electrical insulation materials, and plastics recycling.

ILKKA RYTÖLUOTO received the M.Sc. (Tech.) and Ph.D. degrees in electrical engineering from Tampere University (TAU), Tampere, Finland, in 2011 and 2016, respectively. From 2011 to 2019, he was with the Research Group on High Voltage Engineering, TAU. Since 2019, he has been working as a Senior Scientist at VTT Technical Research Centre of Finland Ltd. He has more than nine years of experience in the field of high-voltage engineering and dielectric material development, especially in thin biaxially oriented capacitor films and HVDC cable insulation, and several years of experience in polymers processing and characterization. His current research interests include polypropylene-based dielectric nanocomposites for high-voltage dc film capacitors and cables, processing-morphology-electrical property relationships of dielectric and electrically conductive polymeric systems, functional polymer composites, polymer processing and recycling, and biaxially oriented thin film technology.

KARI LAHTI received the M.Sc. and Ph.D. degrees in electrical engineering from the Tampere University of Technology (TUT), in 1994 and 2003, respectively. He currently holds the position of Adjunct Professor at TUT. He has over 25 years of experience in the field of high-voltage engineering. Since 2003, he has been responsible for the High Voltage Laboratory, TUT (since 2019 known as Tampere University, TAU), where he has also been the Head of the Research Group on High Voltage Engineering, since 2013, focusing mainly on various aspects of high-voltage insulation systems. His research interests include high-voltage metrology and testing techniques, surge arresters, nanocomposite insulation systems, environmental testing of HV apparatus, and dielectric characterization of HV insulation systems.

RAFAL ANYSZKA (Member, IEEE) received the master's and Ph.D. degrees from the Lodz University of Technology, Poland, in 2010, conducting research in the field of ceramizable elastomer composites. In 2014, he defended his Ph.D. thesis and started a two-years project at his Alma mater concerning the development of sulphur-organic copolymers and composites on their base. From 2017 to 2018, he was working as a Postdoctoral Researcher with the University of Twente, developing hook-and-loop molecular adhesive systems for new generation elastomers. In 2018, he joined the European GRIDABLE Project focused on silica surface modification for high-voltage dc recyclable insulation materials.

MIKA PAAJANEN received the M.Sc. (Tech.) and D.Sc. (Tech.) degrees in electrical engineering and technical physics from the Tampere University of Technology, in 1995 and 2001, respectively. He has been working with VTT Technical Research Centre of Finland Ltd., since 1996, where he is currently working as a Principal Scientist. His research interests include electromechanical films, electrets, plastic nanocomposites, electrical insulation materials, and plastics recycling.

WILMA DIERKES received the degree in chemistry from Technical University, Hanover, Germany, and the master's degree in environmental science from the Fondation Universitaire Luxembourgeoise, Belgium. After finishing her study, she started to work for the rubber recycling company Rubber Resources BV, Maastricht, The Netherlands. She was in-charge of Research and Development Technical Service, and developed and introduced short recycling loops for production waste back into the original production process. The next step in her career was with the Research and Development Department, Robert Bosch Produktie N.V., Tienen, Belgium, where she developed windshield wipers. Additionally, she was the Head of the Chemical Laboratory and a part of the trouble shooting team in the production facility. In 2001, she started to work for the University of Twente, Enschede. From 2009 to 2013, she also held a part-time Professorship at the Tampere Technical University, Finland. Since she started her research work at the university, she published more than 100 reviewed articles, 12 book chapters, and she holds eight patents. Her key research areas are reinforcing filler technology, with emphasis on silica filler systems, and recycling and re-utilization of elastomers. Other research areas are polymer networks and fiber reinforcement. For about ten years, she was a Board Member of the Dutch Association of Plastics and Rubber Technologists (VKRT) and she was the Chairman of this association, from 2005 to 2014.

ANKE BLUME received the degree in chemistry from the University of Hanover, Germany, in 1993. In the last year of her study, she came in the first contact with rubber during her master thesis. Consequently, she carried out her Ph.D. thesis at the German Institute for Rubber Technology (DIK), which she finished in the mid of November 1995. After nine months of her postdoctoral position at DIK, she started as a member of the Product Development Group Silica, Applied Technology Department, Degussa AG (currently it is Evonik Resource Efficiency GmbH), in September 1996. She worked there in different positions, always related to the development of silica and silane for the use in rubber. Since August 2011, she holds the position as an IP Manager silica and silane for rubber applications. In October 2013, she started as the Head of the Chair of Elastomer Technology and Engineering (ETE), University of Twente, The Netherlands.

• • •